

Plasma Formation and Seeding of R-T Instabilities in Wire Array Z-pinch

S. V. Lebedev, J. P. Chittenden, S.N. Bland, F.N.Beg, A. E. Dangor,
M. G. Haines, S.A.Pikuz*, T.A.Shelkovenko*

The Blackett Laboratory, Imperial College, London SW7 2BZ, U. K.

*P.N.Lebedev Physics Institute RAS, Moscow, 117924, Russia

Recent Z-pinch experiments utilising cylindrical arrangements of fine metallic wires as loads have produced record X-ray powers and efficiencies[1,2]. This has sparked great interest in the ICF community who hope to use the X-rays to energise hohlraums for indirect drive fusion research[3]. It is thought that the power and the rise-time of the generated X-ray pulses are primarily determined by the development of the Rayleigh-Taylor (R-T) instability in the imploding plasma. There is a general understanding that the higher the number of wires in the array, the more symmetric the load and the higher the resultant X-ray power indicating a reduction in the level of R-T, but the development of the instability is not fully understood.

Plasma formation in a wire array is heterogeneous. At the start of the current pulse, there is a dwell time during which very little expansion of plasma is seen around the wires. Once dwell time has elapsed material starts to rapidly ablate from each wire to form a core-corona system[4]: a cold, dense, relatively unionised wire core continually ablates forming a surrounding hot, low density coronal plasma. Initially the cores appear stationary and the $\underline{J} \wedge \underline{B}$ force accelerates coronal plasma from around each core into streams that flow towards the array axis. When the coronal streams stagnate on axis, a column of precursor plasma is produced[5]. The process of core ablation and coronal plasma streaming continues until cores start to accelerate and this is accompanied by the development of a global R-T instability. Once the cores reach the axis, the array stagnates and an X-ray pulse is emitted.

In this paper we present studies of the core-corona system in wire arrays, detailing the development of instabilities in the corona and how these instabilities can be transferred to the cores to seed the global R-T instability. We show how the implosion trajectory of the cores undergoes change with wire number. Finally, the use of 2 concentric arrays, the nested configuration, is examined as a way of reducing R-T.

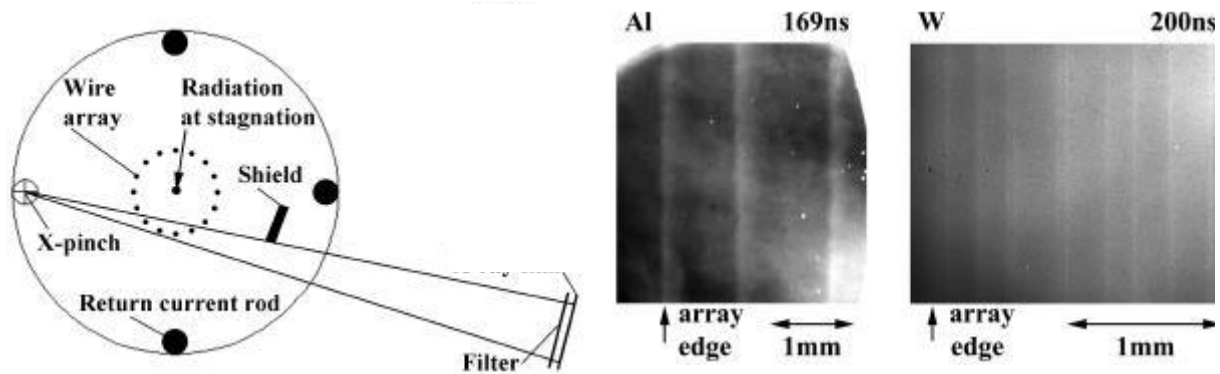


Fig 1: X-ray backlighting set-up

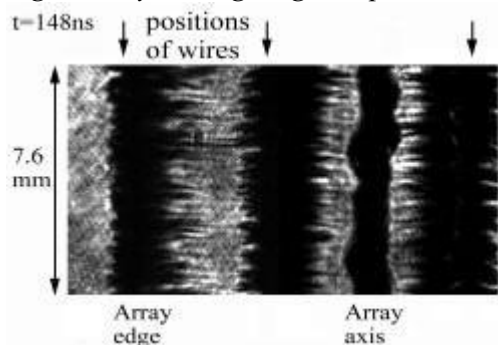


Fig 2: Side-on schlieren photo. of Al array

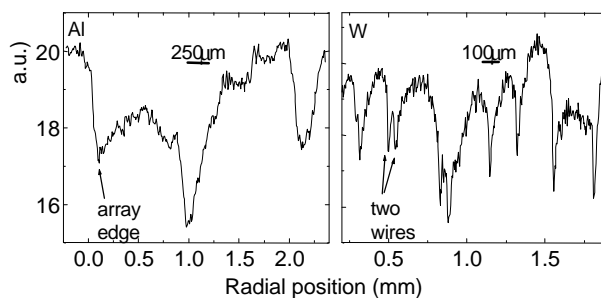


Fig 3: X-ray backlighting images of Al and W arrays and corresponding film densities

Experiments were performed on the MAGPIE generator[6] with current rising to 1MA in 240ns. Arrays were of 16mm diameter and 2.3cm long with 8, 16, 32 or 64 wires (usually 15 μm Al or 4 μm W). The diagnostic set-up included laser probing, a soft X-ray gated camera, a radial optical streak camera and diamond photo-conducting detectors (PCDs), and is described elsewhere[5]. To enable examination of the wire cores, an X-ray backlighting system (imagine flash photography with X-rays) has been developed (fig 1). Two or four crossed wires are placed in one of MAGPIE s current return posts forming an X- [7]. As current flowed through the X-pinch, the cross over point collapses, producing a short duration (<1ns) point source of hard X-rays. A camera on the other side of the array records the image. The timing of the pulse was adjusted by using different diameters of wires in the X-pinch, whilst the probing energy was windowed to 3-5KeV by a titanium filter placed before the film.

Laser probing data shows that after ~60ns, low density coronal plasma from the wires starts streaming towards the array s axis, forming a narrow precursor plasma column at about half the implosion time. The streaming is accompanied by the development of instabilities as seen on schlieren and shadow images (e.g. fig 2). Coronal plasma from each wire within the array seems to demonstrate the same instability wavelength, but the instability is uncorrelated between wires. The wavelength of instability appears unaffected by initial wire diameter and current per wire, but does depend on material: aluminium displays a characteristic wavelength of $\lambda \sim 0.5\text{mm}$, whilst tungsten has $\lambda \sim 0.25\text{mm}$. The large extent of the instability structure in the inward radial direction ($\delta R \sim 5-10\lambda$) indicates the streams are force-free in nature i.e. no further acceleration occurs as they flow towards axis.

Fig 3 shows typical X-ray backlighting images of wire cores at the array edge at ~70% of the implosion time. The cores are still in their original positions. The characteristic sizes of the wire cores are ~0.25mm for aluminium and ~ 0.1mm for tungsten. These sizes are again found to be independent of initial wire diameter and current per wire.

There appears to be a dependence of the coronal instability on the core size. Calculating $ka=(2\pi/\lambda)a$, where λ is taken from the laser probing and a is half of the core size measured by backlighting, produces $ka \sim 1.5$ for both aluminium and tungsten. This implies the size of the region (~the core size) where the formation and acceleration of the coronal plasma takes place determines the development of the instability.

The coronal instability imprints a mass perturbation on the wire core from which it ablated. Once the cores start to accelerate (see later) these perturbations act as a seed for the development of R-T instability. Backlighting images taken at ~80% of the implosion time (e.g. fig 4) clearly show the outer boundary of the cores having the characteristic bubble and spike structure of the R-T instability. The wavelength of the instability is the same as that of the coronal stream (~0.5 mm for the aluminium array in figure 4) and, like the stream, is uncorrelated between cores.

Perturbations in the individual cores can act as a seed towards the global, correlated, R-T instability that develops shortly after they start to accelerate. However, the global instability has a longer wavelength than that in individual cores (e.g. an aluminium array produces a global R-T of $\lambda \sim 2\text{mm}$ [5]). The precise mechanism that determines the global wavelength requires further investigation, but is possibly related to the fact that for a longer wavelength mode the effect of the perturbations in individual cores being out of phase is smaller. Some evidence of the preferential development of a longer wavelength is seen in fig 4, where the amplitude of perturbations is larger if they coincide with perturbations in neighbouring cores.

The implosion dynamics of wire cores were measured by radial optical streak photography. The trajectories found were compared to a 0-D model, which assumes that the array implodes as a hollow plasma cylinder accelerated by the global $\mathbf{J} \wedge \mathbf{B}$ force.

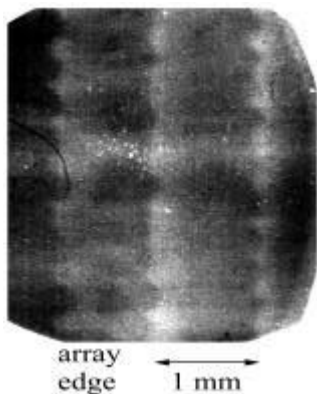


Fig 4: Backlighting image of Al array showing R-T in individual cores.

The implosion trajectories of 8, 16 and 32 aluminium wires and 16, 32 and 64 tungsten wires (fig 5) did not agree with the 0-D model. Instead the cores remained in their initial positions until about 80% of implosion time - the time when the imprint of instabilities on wire cores was detected. The stationary position of the cores can only be understood if no force is applied to them i.e. until this time the current flows mainly in the coronal plasma just around the cores. The sudden acceleration of the cores would then occur at a time when current transferred to them, probably due to the cores being unable to sustain their rate of mass ablation into the coronal plasma. Assuming that all the current is transferred at ~80% of implosion time, a mass fraction of ~ 25-50% remaining in the cores would provide the observed fast implosion.

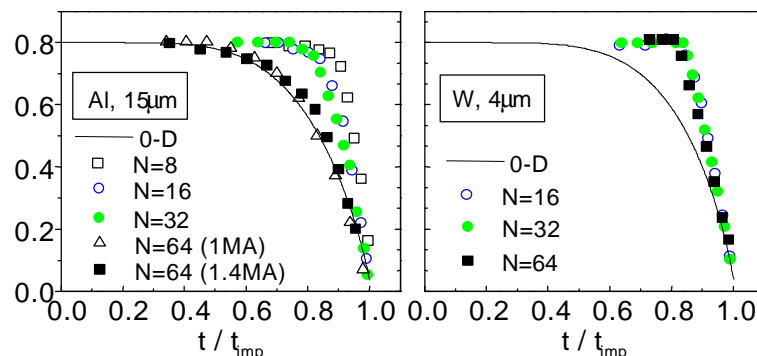


Fig 5: Core implosion trajectories in 15µm Al and 4µm W arrays.

A qualitative change in the implosion dynamics was observed in aluminium arrays when the wire number was increased from 32 to 64 (inter-wire gap decreased from 1.57mm to 0.78mm). The 64 wire trajectory now follows the 0-D model s more closely. A decrease in emission from the precursor was also observed, becoming effectively zero long before stagnation of the array (emission from the precursor in other arrays continued throughout the implosion). This indicates a possible cut off in mass injection towards the axis.

The observed change in the implosion dynamics for aluminium arrays occurred when the ratio between inter-wire separation (0.78mm) and the characteristic size of wire core (0.25mm) became equal to about 3. This could be related to the fact that when the ratio of the inter-wire separation to the wire diameter equals π , the contribution of the private magnetic flux of each wire to the array inductance is zero, and the array inductance becomes equal to that of a thin shell. For tungsten wire arrays, which have a core size a factor of ~2.5 smaller, this could not occur the inter-wire gap reached ~ 0.3mm (which would make the number of wires prohibitively large).

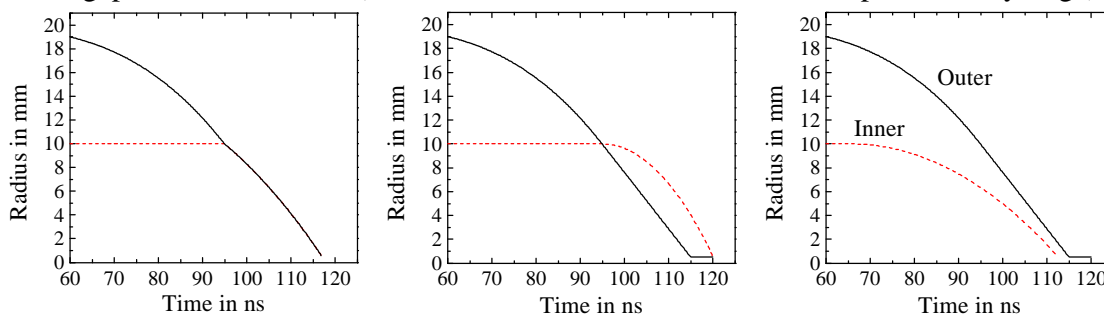


Fig6: 3 modes of nested implosion: a) hydrodynamic collision b) transparent inner c) magnetic buffer

Nested arrays (two concentric arrays, one inside another) have been utilised at Sandia National Labs and led to a 40% increase in X-ray power over single arrays[8]. Three different modes of interaction between the arrays have been suggested (fig 6). The first, hydrodynamic collision mode, assumes that both outer and inner arrays form annular shells. The outer accelerates, and when it hits the inner, any R-T instability annihilates. The combined plasma then implodes too rapidly for any further R-T to grow to excessive levels. The second, transparent mode[9], assumes that the inner array is shielded from current by the outer and remains as discrete wires. Plasma from the outer array passes straight through the gaps in the inner array. The current then switches to the inner array and the resulting plasma implodes rapidly onto the outer material that has already reached the axis. The inner implodes so quickly that again the R-T does

not have time to grow to an excessive level. The third, magnetic buffer mode, assumes that some flux is trapped between the arrays and compressed as the outer starts to move. The compressed flux drives in the inner array, and the result is that the outer and inner never collide but, instead, can reach the axis simultaneously.

It is likely that all 3 processes occur in nested configurations, but one process dominates according to the current flowing through, and the number of wires in the inner[10]. A high number of wires or expansion of its wires by current leads to a high degree of momentum transfer from the outer to the inner and a mostly hydrodynamic collision. A low number of wires with little current flowing through them produces an implosion dominated by current transfer.

Our nested work on MAGPIE has concentrated on isolating the transparent inner mode. To achieve this, a special nested array, the high-L array, has been developed (fig 7). The outer array is identical to the single 16 wire 15µm aluminium arrays used in the previous experiments. The inner array was half the diameter of the outer, again used 16 wires of 15µm aluminium, but was ~3 x the length, increasing its inductance and limiting the current flowing through it. To illustrate the difference in current flow, fig 8 shows 2 shadowgrams taken at the same time - one from a normal nested array, the other from the high L. No measurable expansion is seen from the inner wires of the high-L.

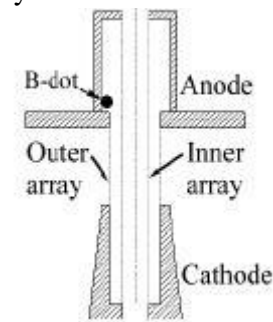


Fig7: The High-L array

Radial optical streaks were again used to study the array dynamics (fig9). The outer arrays trajectory was much the same as that of a single 16 wire array, with the cores remaining in place until ~80% of a single array implosion time and then accelerating inwards. The inner array remained stationary before the outer passed by, and immediately afterwards its velocity was still zero indicating no momentum transfer from outer to inner. The inner then started to accelerate towards the axis, its trajectory closely following the 0-D model assuming all the current was flowing through the central 2.3cm section.

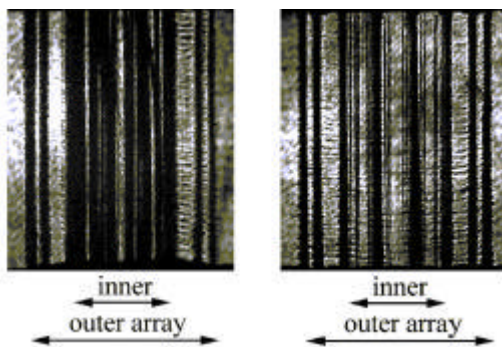


Fig 8: Shadowgrams of a normal array (left) and the high-L array (right)

Soft X-ray emission, monitored by a PCD detector filtered to look at ~180-290eV, is shown in fig10 with a comparison to a single array. The main X-ray pulse of the nested array corresponds to the stagnation of the inner array. The single array had a pulse rise time of ~40ns, but that of the nested was only ~10ns even though the total implosion time was longer due to the R-T in the inner having less time to grow.

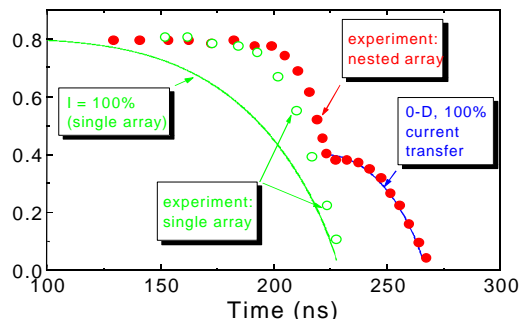


Fig 9: Implosion trajectories of High-L nested array

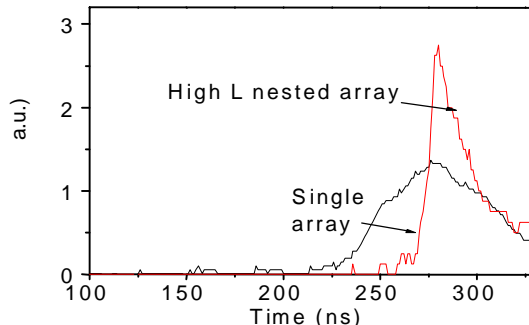


Fig 10: Soft X-ray signals from high-L nested array and single 16 wire array

1. T.W.L. Sanford et al, Phys. Rev. Lett. **77**, 5063 (1996).
2. C. Deeney et al., Phys. Rev. E **56**, 5945 (1997).
3. M.K. Matzen, Phys. Plasmas **4**, 1519 (1997).
4. S.V. Lebedev et al., Phys. Rev. Lett, to be published.
5. S.V. Lebedev et al., Phys. Plasmas **6**, 2016 (1999).
6. I.H. Mitchell et al., Rev. Sci. Instr. **67**, 1533 (1996).
7. T.Shelkovenko et al, Rev. Sci. Instr **70**, 667 (1999).
8. C. Deeney et al., Phys. Rev. Lett. **81**, 4883 (1998).
9. J.Davis et al, Appl. Phys. Lett. **70**, 170 (1997).
10. J.P. Chittenden et al., Phys. Rev. Lett, submitted.